Multi-antenna Non-coherent Detection of Ambient Backscatter under Time-Selective Fading

J. Kartheek Devineni and Harpreet S. Dhillon

***Abstract*—Due to their inherent ability to operate without the channel state information (CSI), non-coherent receivers are highly suitable for ambient backscatter devices, allowing them to co-exist alongside the non-cooperative primary users. In this work, we analyze the performance of an ambient backscatter system employing non-coherent detection in a time-selective fading channel (modeled using the first order autoregressive (AR) process). We characterize the bit error rate (BER) of a multi-antenna (MA) receiver by deriving the expression for antenna gain achievable after the direct link (DL) cancellation. In addition, the analysis also captures the additional angular resolution in a MA receiver with more than two antennas, which allows us to ensure reasonable performance even when the angles of arrival (AoAs) of the DL and backscatter link (BL) are almost similar.**

***Index Terms*—Ambient backscatter, non-coherent detection, auto-regressive model, time-selective fading, bit error rate.**

I. Introduction

Ambient backscatter has emerged as a promising technology for the modern wireless networks due to its enormous potential in supporting numerous applications for the Internet-of-Things (IoT) paradigm [1]. Given the wide scope of these applications, it is natural to expect a variety of deployment scenarios for the backscatter devices. If the underlying statistical conditions for the scenarios are fundamentally different, a receiver optimized to work well in one scenario may not work well for the others. In the context of this work, the receiver optimized for slowly-varying channels, assuming the knowledge of the CSI, may not work well in fast-varying channels due to the non-availability of CSI in those scenarios. Since vehicular networks offer potential use cases for backscatter communications, it is imperative to separately investigate the performance of the system under such fast-varying channels. As will be discussed shortly, this case has not received much attention in the literature (which has mostly focused on slow fading scenarios) [1]. Further, since channel acquisition is complicated in time-selective channels, non-coherent detection is an attractive choice for this setup. Therefore, the main aim of this work is to investigate the BER performance of a non-coherent receiver under a time-selective fading channel.

A. Related Work

The existing literature on non-coherent ambient backscatter is very limited, mainly dealing with slow fading channels modeled under the assumption of block fading [2]–[5]. The maximum-likelihood (ML) detection of a non-coherent ambient backscatter system is analyzed in [2]. Meanwhile in [3], a non-coherent detector is designed to avoid the DL interference by transmitting over the null sub-carriers in orthogonal frequency division multiplexing (OFDM). Blind channel estimation techniques for the ambient backscatter setup are investigated in [4], [5]. The performance of these blind estimation techniques depend on their convergence rate, and hence may not be suitable for time-selective fading. These previous studies in [2]–[5], however, do not jointly investigate the non-coherent detection and time-selective fading. Perhaps the most relevant prior art is our own work [6], where we analyzed non-coherent detection for a dual-antenna receiver under the assumption of independent fading across the ambient symbols. However, the current paper expands the scope of this problem significantly by considering a general multi-antenna receiver and a time-selective fading channel. As discussed shortly, the inclusion of general multi-antenna setting yields many insights that are not quite possible with a restrictive dual-antenna setting.

B. Contributions

In our non-coherent backscatter setup, the time-selective fading channel is modeled as a first order AR process, and the multi-antenna receiver is considered to have an arbitrary number of antennas. The receiver architecture derived using the direct averaging of the received signal samples is easier to implement, while being analytically tractable. The main contributions of our work can be summarized as follows:

1) The joint treatment of non-coherent detection and time-selective fading for an ambient backscatter system,
2) The DL cancellation and the subsequent scalar detection problem for a general antenna receiver.
3) The derivation of the closed form expression for antenna gain and the additional discussion on angular resolution achievable with antenna elements more than two.

To improve the BER performance of the system, the receiver performs the DL cancellation and the subsequent symbol detection by tracking the AoAs of the DL and BL links, which are large scale parameters. In addition to DL cancellation, multiple antennas can be used to obtain antenna gain which improves the BER of the system. Further, it is possible to operate this system even for similar AoAs of the two links, due to the additional angular resolution achieved when the number of receive antennas are higher than two. Also, the average BER is observed to improve with increasing time-domain correlation of the fading, while it reaches an asymptotic value with the increasing sample-size.

J. K. Devineni and H. S. Dhillon are with Wireless@VT, Department of ECE, Virginia Tech, Blacksburg, VA (email: kartheekdj@vt.edu and hdhillon@vt.edu).
This work was supported by U.S. NSF under Grants CNS-1814477 and CPS-1739642.

II. System Model

A. System Setup and Channel Model

The backscatter system in our current setup has three devices: ambient power source (PS), backscatter transmitter (BTx), and receiver (Rx), as illustrated in Fig. 1a. The channel considered in the work is flat Rayleigh faded whose coherence time is of the order of duration of each ambient symbol, with spatial correlation at the Rx. The received signal is composed of two elements, the DL coming from the ambient PS, and the BL reflected from the BTx, with their respective AoAs given by θ_1 and θ_2. Both the PS and BTx can be in motion, due to which the channel gain of the three links (including the link from PS to BTx) will be changing with time. As shown in [7], ambient backscatter can achieve communication with a far away receiver like BS if the PS is not too far from the BTx and the receiver can find a way to separate the two links, which is the primary motivation for the setup shown in Fig 1a. Emerging applications that motivate the consideration of time-selective fading channels for ambient backscatter include smart fabrics where tags/sensors are integrated into garments for monitoring vital signs [8], and smart roads with sensors deployed on the traffic signs. The impulse response of the channel at Rx, corresponding to the DL and BL links, in terms of the dominant non-line-of-sight (NLOS) path and the Rx array response can be given by [9], [10]:

$$\mathbf{h}(t) = \underbrace{\sum_{n=1}^{N} c_n e^{j\phi_n - j2\pi c\tau_n/\lambda + j2\pi f_d \cos\psi_n t}}_{h_0(t)} \mathbf{a}(\theta)\delta\left(t-\bar{\tau}\right), \quad (1)$$

where the NLOS path can be assumed to be a combination of N independent and non-resolvable sub-paths due to the local scatterers around the transmitter. The nth sub-path is characterized by the gain c_n, the phase offset ϕ_n, the time delay τ_n, the maximum Doppler spread (DS) f_d, and the angle of departure (AoD) ψ_n at the transmitter. In the equation, δ represents the delta function while $\bar{\tau}$ is the mean of the individual delays τ_n of the sub-paths. The remaining parameters $\mathbf{a}(.)$ and θ are the Rx array response vector, and AoA of the NLOS path, respectively. The phase offset ϕ_n of each sub-path is uniformly distributed over $[0, 2\pi)$, and the additional phase offset resulting from the path-delay τ_n can also be shown to be uniformly distributed over $[0, 2\pi)$ since the frequency of operation is very high. Applying the central limit theorem (CLT) to the N sub-paths, the magnitude of the variable $h_0(t)$ can be shown to follow Rayleigh distribution. This channel environment is illustrated in Fig. 1b. The channel described here is valid when one of the PS or BTx or both are mobile, and the receiver is located above the rooftops (such as BS) resulting in spatial correlation across the antennas. The channel of the PS-BTx link will be similar to $h_0(t)$ with additional DS coming from the local scatterers around BTx. The receiver of this system makes use of the fact that the varying rate of the AoA of the links is much slower compared to that of $h_0(t)$ [11], and thereby tracks it to improve the BER of the system.

The auto-correlation function (ACF) of the fading process for the DL and BL links is given by

$$\mathbb{E}_{\theta_n,\tau_n,\bar{\psi}}\left[h_0(t)h_0^*(t+t_d)\right] = J_0(2\pi f_d t_d). \quad (2)$$

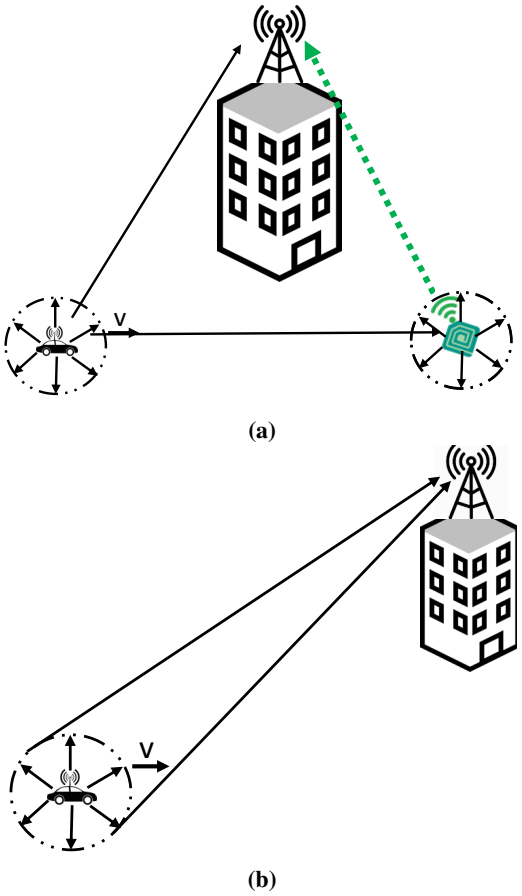

Fig. 1: (a) System model for the ambient backscatter setup, and (b) Illustration of the time-selective fading channel.

This result obtained under the assumption of uniformly distributed azimuthal AoD and unit sum energy of the sub-paths is known as Clarke's reference model. Similarly, the ACF for the PS-BTx link is given by $J_0(2\pi f_d t_d)J_0(2\pi a f_d t_d)$, where a is the ratio of the DS at BTx and PS. To simplify the analysis, the time-selective fading channel in our work is modeled as a first order AR process, and the fading gain corresponding to each signal sample can be represented as [12], [13]:

$$h[n] = \rho\, h[n-1] + \sqrt{1-\rho^2}\, g[n], \quad (3)$$

where $h[n]$ and $h[n-1]$ are the channel gains in the current and previous time periods, $g[n]$ is the complex white Gaussian noise process with variance σ_h^2, and $\rho \in [0, 1)$ is the correlation between the fading coefficients of the consecutive symbols. Depending on the link, the correlation factor ρ is given by either $J_0(2\pi f_d T_s)$ or $J_0(2\pi f_d T_s)J_0(2\pi a f_d T_s)$, where T_s is the symbol duration. The value of ρ determines the rate at which the current channel coefficient de-correlates over time. Interested readers can refer to [14] for additional details on the system setup and the channel model.

B. Signal Model

Since the data rate of most IoT applications is rather small, it is reasonable to assume that the data rate of backscatter is lower compared to that of the ambient symbols. Under this assumption, a single variable is enough to represent the

backscatter data for a signal sample set of size N. The signal at the multi-antenna receiver with $M_r \geq 2$ is given by:

$$\mathbf{y}[n]=\begin{bmatrix} y_0[n] \\ y_1[n] \\ \vdots \\ y_{M_r-1}[n] \end{bmatrix} = h_r[n]\begin{bmatrix} 1 \\ e^{j\phi_1} \\ \vdots \\ e^{j(M_r-1)\phi_1} \end{bmatrix} x[n] + \alpha b\, h_b[n]h_t[n]\begin{bmatrix} 1 \\ e^{j\phi_2} \\ \vdots \\ e^{j(M_r-1)\phi_2} \end{bmatrix} x[n] + \begin{bmatrix} w_0[n] \\ w_1[n] \\ \vdots \\ w_{M_r-1}[n] \end{bmatrix}, \quad (4)$$

where $x[n]$ is the ambient symbol sequence in complex baseband, $w[n]$ is the additive complex Gaussian noise, $h_r[n], h_b[n]$ and $h_t[n]$ are i.i.d. zero mean complex Gaussian channel coefficients with variance σ_h^2, b is the backscatter data, α is related to the parameter Γ_1 (the reflection coefficient of the tag when bit '1' is transmitted) of the BTx node, and the phase offset ϕ_i between consecutive antenna elements for each link in a linear uniform antenna array is given by $\frac{2\pi}{\lambda} d \cos\theta_i$. The channel coefficients $h_r[n], h_b[n]$ and $h_t[n]$ are modeled using the AR process of order 1, each having a different correlation factor given by ρ_r, ρ_b and ρ_t, respectively. Since non-coherent detection does not require the CSI, the channel gains $h_r[n], h_b[n]$ and $h_t[n]$ are unknown at the Rx.

The null and alternate hypotheses of the binary hypothesis testing problem are denoted as $\mathcal{H}_0$ and $\mathcal{H}_1$, respectively. The BTx modulates the backscatter data using the binary on-off keying (OOK) scheme. As is generally the case, the ambient symbol sequence $x[n]$ is assumed to be i.i.d., with unit energy on average. We also assume that the noise energy σ_n^2, the average channel energy σ_h^2, and the correlation factors ρ_r, ρ_b, and ρ_t are known at the receiver. In fact, they can be perfectly estimated with a long observation interval under the assumption that they remain constant, which is true as they are large-scale parameters. The test statistic (TS) for the signal detection is given by the mean of the received signal samples, and can be mathematically expressed as $Z = \frac{1}{N}\sum_{n=1}^{N} y[n]$. In the expanded version of the work, this receiver architecture is shown to be robust to errors in symbol timing synchronization, which is one of the main reasons for adopting it [14].

III. Signal Detection and Bit Error Rate

In this section, we first discuss the proposed DL cancellation technique, then derive the conditional distributions of the resultant signal, and ultimately the BER of the receiver.

A. Effective Signal and Antenna Gain

The signals impinging on the neighboring antenna elements are phase shifted versions of the signal at the first antenna in addition to the independent additive noise. The interference of the DL can be canceled by reversing the DL phase offset at each antenna starting from the second element, and subtracting the resultant signal with that at the first antenna as follows:

$$\tilde{\mathbf{y}}[n] = \begin{bmatrix} e^{-j\phi_1} y_1[n] - y_0[n] \\ \vdots \\ e^{-j(M_r-1)\phi_1} y_{M_r-1}[n] - y_0[n] \end{bmatrix}$$

$$= \tilde{\mathbf{a}}\, \alpha b\, h_b[n]h_t[n]x[n] + \tilde{\mathbf{w}}[n], \quad (5)$$

where the resultant vectors $\tilde{\mathbf{a}}$ and $\tilde{\mathbf{w}}[n]$ are given by:

$$\tilde{\mathbf{a}} = \begin{bmatrix} 2\sin(\frac{\phi_2-\phi_1}{2})e^{j(\frac{\phi_2-\phi_1}{2})} \\ \vdots \\ 2\sin(M_r-1)(\frac{\phi_2-\phi_1}{2})e^{j(M_r-1)(\frac{\phi_2-\phi_1}{2})} \end{bmatrix},$$

$$\tilde{\mathbf{w}}[n] = \begin{bmatrix} e^{-j\phi_1} w_1[n] - w_0[n] \\ \vdots \\ e^{-j(M_r-1)\phi_1} w_{M_r-1}[n] - w_0[n] \end{bmatrix}. \quad (6)$$

The covariance matrix of the resultant noise vector $\tilde{\mathbf{w}}[n]$ is:

$$\mathbf{K}_{\tilde{\mathbf{W}}} = \sigma_n^2 \hat{\mathbf{K}}_{\tilde{\mathbf{W}}}, \quad \text{where } \hat{\mathbf{K}}_{\tilde{\mathbf{W}}} = \begin{bmatrix} 2 & 1 & \dots & 1 \\ \vdots & \vdots & \ddots & \vdots \\ 1 & 1 & \dots & 2 \end{bmatrix}, \quad (7)$$

which means that the resultant noise after the DL cancellation is correlated. The vector detection problem can be converted to scalar detection by appropriately designing the weight vector. The effective scalar signal samples for the averaging operation are obtained by the following steps: 1) Whiten the additive noise with the linear transformation $\hat{\mathbf{K}}_{\tilde{\mathbf{W}}}^{-\frac{1}{2}}$, and 2) Project the output of the first step along the direction of resultant antenna response $\hat{\mathbf{K}}_{\tilde{\mathbf{W}}}^{-\frac{1}{2}}\tilde{\mathbf{a}}$. The combined weight vector of the two operations is $\mathbf{r} = \frac{\hat{\mathbf{K}}_{\tilde{\mathbf{W}}}^{-1}\tilde{\mathbf{a}}}{|\hat{\mathbf{K}}_{\tilde{\mathbf{W}}}^{-\frac{1}{2}}\tilde{\mathbf{a}}|}$, and the effective signal after these steps is:

$$y_{\text{eff}}[n] = \mathbf{r}^*\tilde{\mathbf{a}}\alpha b\, h_b[n]h_t[n]x[n] + \mathbf{r}^*\tilde{\mathbf{w}}[n]. \quad (8)$$

Henceforth, the amplitude gain $\mathbf{r}^*\tilde{\mathbf{a}}$ and the effective additive noise $\mathbf{r}^*\tilde{\mathbf{w}}[n]$ in (8) are denoted as μ and $v[n]$, respectively. The antenna gain (SNR) due to multiple antennas is given by $\tilde{\mathbf{a}}^*\hat{\mathbf{K}}_{\tilde{\mathbf{W}}}^{-1}\tilde{\mathbf{a}}$. This procedure to generate the scalar sample $y_{\text{eff}}[n]$ maximizes the SNR of the signal, and in addition the resultant sample $y_{\text{eff}}[n]$ is a sufficient statistic for the latter detection procedure. It can be further shown that this procedure also minimizes the mean square error for the signal estimation, and hence is known as linear minimum mean squared error estimation (MMSE) [15]. The phase-offset components $e^{j\phi_1}$ and $e^{j\phi_2}$ of the two links can be estimated from the received signal by formulating a parameter estimation problem. However, this is beyond the scope of the current work, and hence they are assumed to be perfectly known at the receiver. The sample average $Z = \frac{1}{N}\sum_{n=1}^{N} y_{\text{eff}}[n]$ is used as the new test statistic.

Lemma 1. *The antenna gain $G = \tilde{\mathbf{a}}^*\hat{\mathbf{K}}_{\tilde{\mathbf{W}}}^{-1}\tilde{\mathbf{a}}$ of the receiver is:*

$$G = M_r - \frac{1}{M_r} - \frac{2}{M_r}\frac{\sin((M_r-1)\frac{\phi_2-\phi_1}{2})}{\sin(\frac{\phi_2-\phi_1}{2})}\cos(\frac{M_r}{2}(\phi_2-\phi_1)) - \frac{1}{M_r}\frac{\sin^2((M_r-1)\frac{\phi_2-\phi_1}{2})}{\sin^2(\frac{\phi_2-\phi_1}{2})}. \quad (9)$$

Proof: See Appendix A. ∎

For notational simplicity, the antenna gain is represented as a single variable G without any input arguments even though it is a function of the two phase offsets (and hence the AoAs).

Remark 1. *The antenna gain for a dual-antenna Rx simplifies to $G = 2\sin^2(\frac{\phi_2-\phi_1}{2})$, which is zero when the AoAs of the DL and BL links are almost the same. On the other hand, the antenna gain G for a Rx with $M_r > 2$ equals $(1-\frac{1}{M_r})(M_r-2)$,*

which is non-zero even when the two AoAs are almost the same (in a limiting sense). Hence, additional angular resolution is obtained with $M_r > 2$, which is beneficial for the scenarios where the AoAs of the DL and BL links are very similar.

B. Conditional Distributions and Bit Error Rate

Now, we can derive the conditional distributions from the effective signal, and then the average BER of the receiver.

Lemma 2. *The conditional PDFs of Z for the two hypotheses $\mathcal{H}_0$ and $\mathcal{H}_1$ are given by*

$$\mathcal{H}_i : Z \sim \mathcal{CN}\left(0, \mathrm{Var}_i\right), \tag{10}$$

where $\mathrm{Var}_0 = \frac{\sigma_n^2}{N}$ *and*

$$\mathrm{Var}_1 = \frac{G|\alpha|^2\sigma_h^4\left\{\mathbb{E}\left[|X|^2\right]+\frac{2\rho_t\rho_b}{1-\rho_t\rho_b}\left(1-\frac{1-\rho_t^N\rho_b^N}{N(1-\rho_t\rho_b)}\right)|\mathbb{E}[X]|^2\right\}+\sigma_n^2}{N}.$$

Proof: See Appendix B. ∎

Theorem 1. *The average BER of the receiver is given by:*

$$P(e) = \int_{-\pi}^{\pi}\int_{-\pi}^{\pi}\frac{1}{8\pi^2}\left(1 - e^{-\frac{T}{\mathrm{Var}_1}} + e^{-\frac{T}{\mathrm{Var}_0}}\right)\mathrm{d}\theta_1\mathrm{d}\theta_2, \tag{11}$$

where $T = \ln(\frac{\mathrm{Var}_1}{\mathrm{Var}_0})\frac{\mathrm{Var}_1\mathrm{Var}_0}{\mathrm{Var}_1-\mathrm{Var}_0}$ *is the optimal detection threshold.*

Proof: See Appendix C. ∎

Asymptotic BER: Ratio of the variances of $\mathcal{H}_0$ and $\mathcal{H}_1$ is:

$$K = 1 + G|\alpha|^2\sigma_h^4\{1 + \frac{2\rho_t\rho_b}{1-\rho_t\rho_b}(1 - \frac{1-\rho_t^N\rho_b^N}{N(1-\rho_t\rho_b)})\frac{|\mathbb{E}\left[X\right]|^2}{\mathbb{E}\left[|X|^2\right]}\}\mathrm{SNR}. \tag{12}$$

From this, the asymptotic conditional BER as $\mathrm{SNR} \to \infty$ is:

$$P^{\mathrm{asym}}(e|\phi_1,\phi_2) \overset{(a)}{=} \frac{1}{2}(1 - K^{\frac{-1}{K-1}} + \frac{1}{K}^{\frac{1}{1-\frac{1}{K}}}) \overset{(b)}{=} 0, \tag{13}$$

where (a) results from substituting the expression for T, and replacing $\frac{\mathrm{Var}_1}{\mathrm{Var}_0}$ with K defined in (12), and (b) follows from the standard limit $\lim_{x\to\infty}(x)^{-1/x-1} = 1$, and $\frac{1}{K} \to 0$ as $\mathrm{SNR} \to \infty$. It should be noted that the asymptotic value of K when $N \to \infty$ is non-zero. Hence, the BER does not converge to 0.5 as $N \to \infty$, even though the individual variances go to zero.

Remark 2. *In case of fast-fading, where the fading gains are independent across the ambient symbols, the average BER is only dependent on the expected value of the energy of ambient symbol. This special case concurs with our analysis in [6]. Alternatively, if the mean value of the ambient symbol is zero (valid for most modulation schemes), then again the average BER is dependent only on the expected value of the energy. Lastly, it can be inferred from the BER expression that the average BER is a decreasing function of the correlation factor.*

The symbol timing recovery is an important component of the ambient backscatter system, which is omitted in this document due to space constraints. Interested readers can refer to the expanded version for additional details [14].

IV. Numerical Results and Discussion

In this section, the accuracy of our analysis is verified by comparing with Monte-Carlo simulations. The reflection coefficient Γ_1 is configured appropriately to set the parameter α that will result in a signal attenuation of 1.1 dB, and the variance

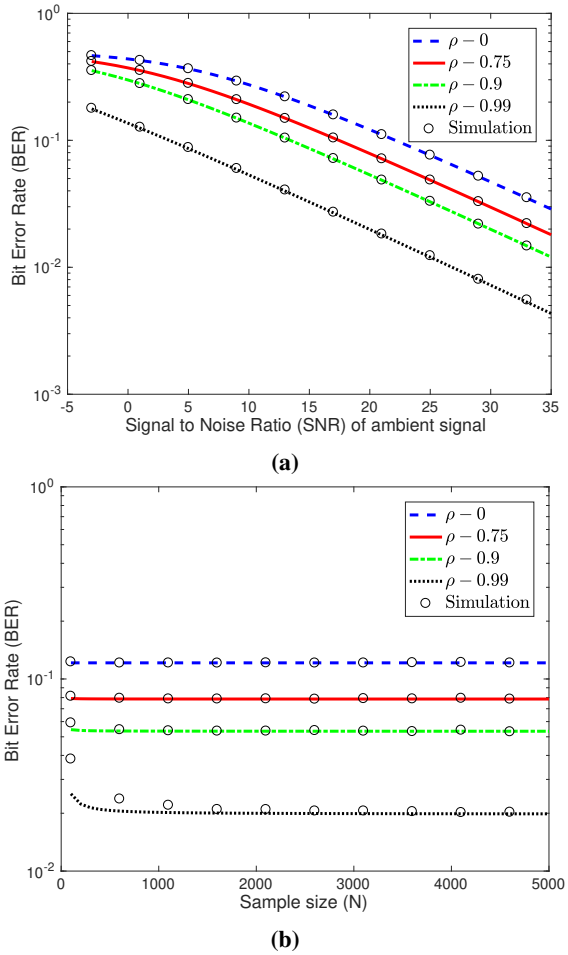

Fig. 2: (a) BER vs SNR comparison of the Rx with $M_r = 2$ for varying correlation ρ and $N = 5000$, (b) BER vs N comparison of the Rx with $M_r = 2$ for varying correlation ρ with $\mathrm{SNR} = 20\,\mathrm{dB}$.

of the fading gain σ_h^2 is set to 1. Unless explicitly specified for the particular plot, the values of ρ_r, ρ_b and ρ_t are all considered equal and represented as ρ. The BER performance with increasing SNR for different values of ρ is shown in Fig. 2a, where it can be seen that the BER improves with increasing ρ value. Likewise, the BER performance with increasing N for varying ρ is shown in Fig. 2b, and interestingly the BER increases and saturates quickly with increasing N. However, as expected, there is an increasing mismatch between the simulated and theoretical results of BER at lower values of N as the ρ value is increased. This mismatch occurs due to the need of a larger sample-size N for the averaging operation, so that the simulation and theoretical results converge with increasing ρ. The antenna gain with additional antennas is presented in Fig. 3a, that shows around 8 dB gain with the doubling of antennas. The simulation result for the analysis in Remark 1, regarding the additional angular resolution achievable with receive antennas beyond two, is shown in Fig. 3b. For this comparison, one can assume the AoA θ_1 of the DL to be uniformly distributed between $(-\pi, \pi]$, and the AoA θ_2 of the BL to be uniformly distributed with mean θ_1 and width $\Delta\theta = 10°$. The results demonstrate that while the BER of the dual-antenna Rx is close to 0.5, an antenna gain of around 9 dB is achieved with the doubling of antennas.

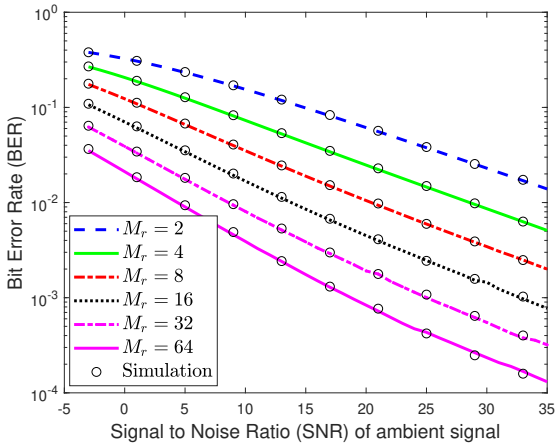

(a)

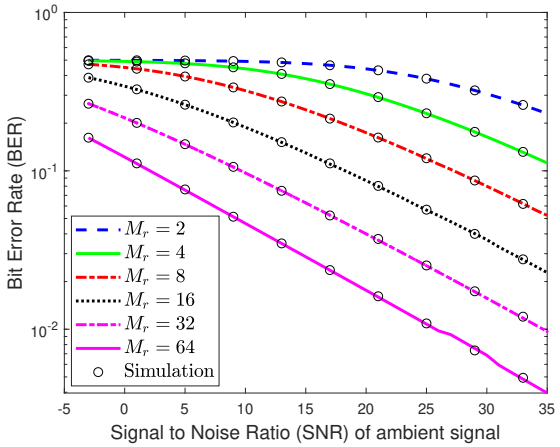

(b)

Fig. 3: BER vs SNR comparison for changing antenna elements M_r at the receiver with $\rho_r = 0.5, \rho_b = 0.75, \rho_t = 0.38$ and $N = 2000$: (a) uniformly distributed AoAs, and (b) narrowly distributed AoAs.

V. Conclusion

In this paper, we have studied the performance of an ambient backscatter system by studying the design and BER of a multi-antenna non-coherent detector under time-selective fading channels. The receiver architecture configured using the direct averages of the received signal samples is much simpler to implement, and also lends tractability to the asymptotic analysis. Using multiple antennas at the receiver, the strong DL interference is eliminated and an SNR gain is achieved by appropriately processing the signal, thereby resulting in a good BER performance. We have also demonstrated, through both analytical and numerical results, the additional angular resolution achievable with more than two receive antennas, which benefits the scenarios where the DL and BL AoAs are very similar. Though the BER in the time-selective fading improves with increasing signal sample-size, it saturates to an asymptotic value. Additionally, the BER is observed to improve with increasing temporal-correlation of the fading channel.

Appendix

A. Proof of Lemma 1

The antenna gain $\tilde{\mathbf{a}}^* \hat{\mathbf{K}}_{\tilde{\mathbf{W}}}^{-1} \tilde{\mathbf{a}}$ of the receiver is dependent on the inverse of the matrix $\hat{\mathbf{K}}_{\tilde{\mathbf{W}}}$, for which closed-form expression can be obtained. The matrix $\hat{\mathbf{K}}_{\tilde{\mathbf{W}}}$ can be re-written as:

$$\hat{\mathbf{K}}_{\tilde{\mathbf{W}}} = \mathbf{I}_{M_r-1} + \mathbf{J}_{M_r-1},$$

where $\mathbf{I}_{M_r-1}$ is an identity matrix, and $\mathbf{J}_{M_r-1}$ is an all-ones matrix whose rank will be one. Therefore, $\mathbf{J}_{M_r-1}$ can be simplified using singular value decomposition (SVD) as $\mathbf{u}_1 \sigma_1 \mathbf{v}_1^T$, where the unitary matrices are given by $\mathbf{u}_1 = \mathbf{v}_1 = \frac{-1}{\sqrt{M_r-1}} \begin{bmatrix} 1 & 1 & \dots & 1 \end{bmatrix}^T$, and the non-zero singular value $\sigma_1 = M_r - 1$. Due to the symmetry, this can be re-written in the form $\mathbf{J}_{M_r-1} = \mathbf{u}\mathbf{u}^T$, where $\mathbf{u} = \begin{bmatrix} 1 & 1 & \dots & 1 \end{bmatrix}^T$. Now, according to the Sherman-Morrison formula [16], inverse of the sum of a invertible matrix $\mathbf{A}$ and the outer product $\mathbf{u}\mathbf{v}^T$ is given by $\left(\mathbf{A} + \mathbf{u}\mathbf{v}^T\right)^{-1} = \mathbf{A}^{-1} - \dfrac{\mathbf{A}^{-1}\mathbf{u}\mathbf{v}^T\mathbf{A}^{-1}}{1 + \mathbf{v}^T\mathbf{A}^{-1}\mathbf{u}}$. Using this, the inverse of the matrix $\hat{\mathbf{K}}_{\tilde{\mathbf{W}}}$ can be derived as:

$$\hat{\mathbf{K}}_{\tilde{\mathbf{W}}}^{-1} = \mathbf{I}_{M_r-1} - \frac{\mathbf{u}\mathbf{u}^T}{1 + \mathbf{u}^T\mathbf{u}} = \mathbf{I}_{M_r-1} - \frac{\mathbf{J}_{M_r-1}}{M_r}. \tag{14}$$

The expression of the SNR gain can be simplified as:

$$\tilde{\mathbf{a}}^* \hat{\mathbf{K}}_{\tilde{\mathbf{W}}}^{-1} \tilde{\mathbf{a}} = \begin{bmatrix} e^{-j(\phi_2-\phi_1)} - 1 & \dots & e^{-j(M_r-1)(\phi_2-\phi_1)} - 1 \end{bmatrix}$$
$$\begin{bmatrix} \frac{M_r-1}{M_r} & \frac{-1}{M_r} & \dots & \frac{-1}{M_r} \\ \vdots & \vdots & \ddots & \vdots \\ \frac{-1}{M_r} & \frac{-1}{M_r} & \dots & \frac{M_r-1}{M_r} \end{bmatrix} \begin{bmatrix} e^{j(\phi_2-\phi_1)} - 1 \\ \vdots \\ e^{j(M_r-1)(\phi_2-\phi_1)} - 1 \end{bmatrix}$$
$$= -S_{M_r-1} - S_{M_r-1}^* - \frac{S_{M_r-1} S_{M_r-1}^*}{M_r},$$

where $S_{M_r-1} = \sum_{i=1}^{M_r-1} \left[e^{ji(\phi_2-\phi_1)} - 1 \right]$ is the summation of all the elements in the weight vector. Since, S_{M_r-1} is a geometric sum it can be simplified, and the sum $S_{M_r-1} + S_{M_r-1}^*$ and product $S_{M_r-1} S_{M_r-1}^*$ can be derived as following:

$$S_{M_r-1} + S_{M_r-1}^* = 2 \frac{\sin((M_r-1)\frac{\phi_2-\phi_1}{2})}{\sin(\frac{\phi_2-\phi_1}{2})} \cos(\frac{M_r}{2}(\phi_2-\phi_1)) - 2(M_r-1)$$

$$S_{M_r-1} S_{M_r-1}^* = \frac{\sin^2((M_r-1)\frac{\phi_2-\phi_1}{2})}{\sin^2(\frac{\phi_2-\phi_1}{2})} + (M_r-1)^2 - 2(M_r-1) \frac{\sin((M_r-1)\frac{\phi_2-\phi_1}{2})}{\sin(\frac{\phi_2-\phi_1}{2})} \cos(\frac{M_r}{2}(\phi_2-\phi_1)).$$

Using these simplifications, the final expression for the SNR gain $G = \tilde{\mathbf{a}}^* \hat{\mathbf{K}}_{\tilde{\mathbf{W}}}^{-1} \tilde{\mathbf{a}}$ can be determined as follows:

$$G = M_r - \frac{1}{M_r} - \frac{2}{M_r} \frac{\sin((M_r-1)\frac{\phi_2-\phi_1}{2})}{\sin(\frac{\phi_2-\phi_1}{2})} \cos(\frac{M_r}{2}(\phi_2-\phi_1)) - \frac{1}{M_r} \frac{\sin^2((M_r-1)\frac{\phi_2-\phi_1}{2})}{\sin^2(\frac{\phi_2-\phi_1}{2})}.$$

B. Proof of Lemma 2

The effective signal $y_{\text{eff}}[n]$, given in (8), under $\mathcal{H}_0$ is a complex Gaussian RV with variance σ_n^2. Hence, the mean Z of the received samples under $\mathcal{H}_0$ is a complex Gaussian RV with variance $\text{Var}_0^{\text{MA}} = \frac{\sigma_n^2}{N}$. On the other hand, observe that when conditioned on the ambient signal $x[n]$ and $h_b[n]$, $y_{\text{eff}}[n]$ under $\mathcal{H}_1$ is a complex Gaussian RV. As a result, the mean of the received samples can also be characterized as a complex Gaussian, *albeit* the samples correlated with one another. The

conditional expectation and variance of an individual sample $y_{\text{eff}}[n]$, and the conditional covariance of any two distinct samples $y_{\text{eff}}[i]$ and $y_{\text{eff}}[j]$ can be evaluated as:

$$\mathbb{E}\left[y_{\text{eff}}[n]\right] = \mu\alpha\, h_b[n]x[n]\mathbb{E}\left[h_t[n]\right] + \mathbb{E}\left[v[n]\right] = 0,$$

$$\text{Var}\left[y_{\text{eff}}[n]\right] = G|\alpha|^2|h_b[n]x[n]|^2\text{Var}\left[h_t[n]\right] + \text{Var}\left[v[n]\right]$$
$$= G|\alpha|^2\sigma_h^2|h_b[n]x[n]|^2 + \sigma_n^2,$$

$$\text{Cov}\left[y_{\text{eff}}[i], y_{\text{eff}}[j]\right] = G|\alpha|^2 h_b[i]h_b^*[j]x[i]x^*[j]\text{Cov}[h_t[i], h_t[j]]$$
$$= G|\alpha|^2\sigma_h^2\rho_t^{|j-i|}h_b[i]h_b^*[j]x[i]x^*[j].$$

The conditional expectation and variance of the mean of samples Z can be evaluated as follows:

$$\mathbb{E}\left[Z\right] = \frac{1}{N}\left(\sum_{n=1}^{N}\mathbb{E}\left[y_{\text{eff}}[n]\right]\right) = 0,$$

$$\text{Var}\left[Z\right] = \frac{1}{N^2}\Big(\sum_{n=1}^{N}\text{Var}\left[y_{\text{eff}}[n]\right] + \sum_{n_1\neq n_2}\text{Cov}\left[y_{\text{eff}}[n_1], y_{\text{eff}}[n_2]\right]\Big)$$
$$= \frac{1}{N}\Big(\sigma_n^2 + G|\alpha|^2\sigma_h^2\underbrace{\frac{1}{N}\sum_{1\leq n_1,n_2\leq N}\rho_t^{|n_1-n_2|}\, h_b[n_1]h_b^*[n_2]x[n_1]x^*[n_2]}_{M_N}\Big).$$

The sequence M_N is a function of the sum variable of the ambient sequence $x[n]$, and can be shown to asymptotically converge to its expectation as below:

$$\mathbb{E}\left[M_N\right] = \frac{1}{N}\mathbb{E}\left[\sum_{1\leq n_1,n_2\leq N}\rho_t^{|n_1-n_2|}\, h_b[n_1]h_b^*[n_2]x[n_1]x^*[n_2]\right]$$
$$\overset{(b)}{=} \sigma_h^2\sum_{1\leq n\leq N}\frac{\mathbb{E}\left[|X|^2\right]}{N} + \sigma_h^2\sum_{n_1\neq n_2}(\rho_t\rho_b)^{|n_1-n_2|}\frac{|\mathbb{E}[X]|^2}{N}$$
$$\overset{(c)}{=} \sigma_h^2\mathbb{E}\left[|X|^2\right] + \sigma_h^2\frac{2\rho_t\rho_b}{1-\rho_t\rho_b}\left(1-\frac{1-\rho_t^N\rho_b^N}{N(1-\rho_t\rho_b)}\right)|\mathbb{E}[X]|^2,$$

where (b) follows from the assumption that the ambient sequence $x[n]$ is i.i.d. and the expectation of $h_b[n_1]h_b^*[n_2]$ which is given by $\sigma_h^2\rho_b^{|n_1-n_2|}$, and (c) follows from the value of summation $\sum_{n_1\neq n_2}(\rho_t\rho_b)^{|n_1-n_2|}$ given in [14, Lemma 1].

The conditional variance of Z can thus be approximated as:

$$\text{Var}\left[Z\right] \approx \frac{1}{N}\left(G|\alpha|^2\sigma_h^2\mathbb{E}\left[M_N\right] + \sigma_n^2\right)$$
$$= \frac{G|\alpha|^2\sigma_h^4}{N}(\mathbb{E}\left[|X|^2\right] + \frac{2\rho_t\rho_b}{1-\rho_t\rho_b}(1-\frac{1-\rho_t^N\rho_b^N}{N(1-\rho_t\rho_b)})|\mathbb{E}\left[X\right]|^2) + \frac{\sigma_n^2}{N}.$$

C. Proof of Theorem 1

The optimal decision rule for the receiver is evaluated through the comparison of the conditional PDFs of the null and alternate hypotheses $\mathcal{H}_0$ and $\mathcal{H}_1$, which is given by [6]:

$$\ln\left[f_{Z|\mathcal{H}_0}(z)\right] \gtrless_1^0 \ln\left[f_{Z|\mathcal{H}_1}(z)\right]$$
$$-\ln\left(\text{Var}_0\right) - \frac{|z|^2}{\text{Var}_0} \gtrless_1^0 -\ln\left(\text{Var}_1\right) - \frac{|z|^2}{\text{Var}_1}$$
$$|z|^2 \gtrless_0^1 \ln\left(\frac{\text{Var}_1}{\text{Var}_0}\right)\frac{\text{Var}_1\text{Var}_0}{\text{Var}_1 - \text{Var}_0},$$

where z is the mean of signal samples. The value of the optimal detection threshold T is given by the decision rule.

The decision rule of the optimal detection is only dependent on $|Z|^2$. The variable $|Z|^2$ is an exponential distributed RV, whose mean parameter equals the variance of the complex Gaussian. Assuming that the prior probabilities of the two hypotheses are equal, the conditional BER can be derived as:

$$P(e|\phi_1,\phi_2) = P(\mathcal{H}_0)P(e|\phi_1,\phi_2,\mathcal{H}_0) + P(\mathcal{H}_1)P(e|\phi_1,\phi_2,\mathcal{H}_1)$$
$$= \frac{1}{2}\left(Pr\left\{|Z|^2 > T|\mathcal{H}_0\right\} + Pr\left\{|Z|^2 < T|\mathcal{H}_1\right\}\right)$$
$$= \frac{1}{2}\left(1 - F_{\text{exp}}\left(T, \text{Var}_0\right) + F_{\text{exp}}\left(T, \text{Var}_1\right)\right)$$
$$= \frac{1}{2} - \frac{1}{2}e^{-\frac{T}{\text{Var}_1}} + \frac{1}{2}e^{-\frac{T}{\text{Var}_0}},$$

where $F_{\text{Exp}}(x,\lambda)$ is the cumulative distribution function of the exponential RV $|Z|^2$. The conditional BER is a function of the phase-offsets of the DL and BL links, and the average BER is obtained by marginalizing the conditional BER over the variables θ_1 and θ_2. The assumption here is that θ_1 and θ_2 are i.i.d. and uniformly distributed over $(-\pi, \pi]$, and the final expression in the result can be obtained by marginalizing over this range of θ_1 and θ_2.

REFERENCES

[1] J. K. Devineni and H. S. Dhillon, "Ambient backscatter systems: Exact average bit error rate under fading channels," *IEEE Trans. Green Commun. and Networking*, vol. 3, no. 1, pp. 11–25, Mar. 2019.

[2] J. Qian, F. Gao, G. Wang, S. Jin, and H. Zhu, "Noncoherent Detections for Ambient Backscatter System," *IEEE Trans. Wireless Commun.*, vol. 16, no. 3, Mar. 2017.

[3] M. A. El Mossallamy, M. Pan, R. Jäntti, K. G. Seddik, G. Y. Li, and Z. Han, "Noncoherent backscatter communications over ambient OFDM signals," *IEEE Trans. Commun.*, 2019.

[4] W. Zhao, G. Wang, S. Atapattu, and B. Ai, "Blind channel estimation in ambient backscatter communication systems with multiple-antenna reader," in *2018 IEEE/CIC Intl. Conf. on Commun. in China (ICCC)*, 2018, pp. 320–324.

[5] H. Guo, Q. Zhang, D. Li, and Y.-C. Liang, "Noncoherent multiantenna receivers for cognitive backscatter system with multiple RF sources," *arXiv preprint, arXiv:1808.04316*, 2018.

[6] J. K. Devineni and H. S. Dhillon, "Non-coherent signal detection and bit error rate for an ambient backscatter link under fast fading," *Proc., IEEE Globecom*, Dec. 2019.

[7] A. Varshney, O. Harms, C. Perez-Penichet, C. Rohner, F. Hermans, and T. Voigt, "Lorea: A backscatter architecture that achieves a long communication range," *Proc., ACM on Embedded Network Sensor Systems (SenSys 17)*, no. 50, Nov. 2017.

[8] A. Wang, V. Iyer, V. Talla, J. R. Smith, and S. Gollakota, "FM backscatter: Enabling connected cities and smart fabrics," in *Symposium on Networked Systems Design and Implementation (NSDI 17)*, 2017, pp. 243–258.

[9] G. Raleigh, S. N. Diggavi, A. F. Naguib, and A. Paulraj, "Characterization of fast fading vector channels for multi-antenna communication systems," in *Proc. of 1994 28th Asilomar Conf. on Signals, Systems and Computers*, vol. 2. IEEE, 1994, pp. 853–857.

[10] A. M. Sayeed, "Deconstructing multiantenna fading channels," *IEEE Trans. Signal Processing*, vol. 50, no. 10, pp. 2563–2579, 2002.

[11] A. Adhikary, H. S. Dhillon, and G. Caire, "Massive-mimo meets hetnet: Interference coordination through spatial blanking," *IEEE J. Sel. Areas Commun.*, vol. 33, no. 6, pp. 1171–1186, 2015.

[12] Z. Liu, X. Ma, and G. B. Giannakis, "Space-time coding and kalman filtering for time-selective fading channels," *IEEE Trans. Commun.*, vol. 50, no. 2, pp. 183–186, 2002.

[13] K. E. Baddour and N. C. Beaulieu, "Autoregressive modeling for fading channel simulation," *IEEE Trans. Wireless Commun.*, vol. 4, no. 4, pp. 1650–1662, 2005.

[14] J. K. Devineni and H. S. Dhillon, "Non-coherent detection and bit error rate for an ambient backscatter link in time-selective fading," *arXiv preprint arXiv:1908.05657*, 2019.

[15] D. Tse and P. Viswanath, "Fundamentals of wireless communication," *Cambridge University Press*, 2005.

[16] W. W. Hager, "Updating the inverse of a matrix," *SIAM review*, vol. 31, no. 2, pp. 221–239, 1989.